Pergamon

Tetrahedron 58 (2002) 757–764

TETRAHEDRON

Non-covalent synthesis of calix[4]arene-capped porphyrins in polar solvents via ionic interactions

Roberto Fiammengo,[a] Peter Timmerman,[a,*] Jurrian Huskens,[a] Kees Versluis,[b] Albert J. R. Heck[b] and David N. Reinhoudt[a,*]

[a]*Laboratory of Supramolecular Chemistry and Technology, MESA*$^+$ *Research Institute, P.O. Box 217, 7500 AE Enschede, The Netherlands*
[b]*Department of Biomolecular Mass Spectrometry, Utrecht Institute for Pharmaceutical Sciences and Bijvoet Center for Biomolecular Research, Utrecht University, Sorbonnelaan 16, 3584 CA Utrecht, The Netherlands*

Received 24 July 2001; revised 28 August 2001; accepted 29 August 2001

Abstract—Non-covalent synthesis of calix[4]arene capped porphyrins can be achieved in polar solvents (up to 45% molar fraction of water) via ionic interaction. Thus tetracationic *meso*-tetrakis(*N*-alkylpyridinium-3-yl) porphyrins **1a–d** and tetra anionic 25,26,27,28-tetrakis(2-ethoxyethoxy)-calix[4]arene tetrasulfonate **2** self-assemble in an entropy driven process in 1:1 stoichiometry with association constants $K_{1\cdot2}$ as high as 10^7 M^{-1} in methanol. The thermodynamic stability remains high even in the presence of competing salts: 10^{-2} M Bu_4NClO_4 (4500 times the concentration of the building blocks) gives a reduction in $K_{1\cdot2}$ of only 10 times. Ternary complexes **1a·2·L** using 1-methylimidazole or pyridine as axial ligands (**L**) have been obtained with **L** residing outside the assembly cavity.

1. Introduction

There are few classes of chemical compounds that have attracted more attention of chemists as metalloporphyrins have done. These compounds play an important role as prosthetic groups in several proteins like hemoglobin,[1] the cytochrome P-450 mono-oxygenase family[2] and peroxidases.[3] Whereas the central metal ion (coordinated to the four pyrrolic nitrogens) is the functional unit in molecular recognition and catalysis, the selectivity in these processes as well as the stability of the systems, is largely due to non-covalent interactions with the surrounding protein structure. Such interactions are possible because of the shielded position of the porphyrin within the pocket of the folded protein backbone.

Synthetic chemists have extensively tried to mimic natural porphyrin systems via covalent modification of the porphyrin periphery, resulting in a multitude of porphyrin structures such as capped, strapped, picnic basket, twin coronet and others.[4–6] A non-covalent approach to the modification of the porphyrin periphery has been attempted via coordination chemistry[7] or via hydrogen-bond interactions[8] generally resulting in multiporphyrin systems. However, little attention has been paid to the use of ionic interactions.[9–11] Among the systems consisting of a single porphyrin unit there are examples of porphyrin–cyclodextrin complexes,[12–14] porphyrins in phosholipid vesicles,[15] porphyrins interacting with other chromophoric units[16] or systems used for sensing purposes.[17] In a preliminary communication we have recently reported on the use of multiple ionic interactions for the self-assembly of cationic zinc(II) *meso*-tetrakis(*N*-alkylpyridinium-3-yl) porphyrins **1a–c** and anionic 25,26,27,28-tetrakis(2-ethoxyethoxy)-calix[4]arene tetrasulfonate[18] **2** (Fig. 1). Here we report detailed information on these self-assembly experiments in solvent mixtures containing as much as 45% of water (molar fraction) using the polar porphyrin derivative **1d**. Moreover, the formation of ternary complexes with nitrogenous bases that coordinate to the zinc atom of the ionic complexes is described.

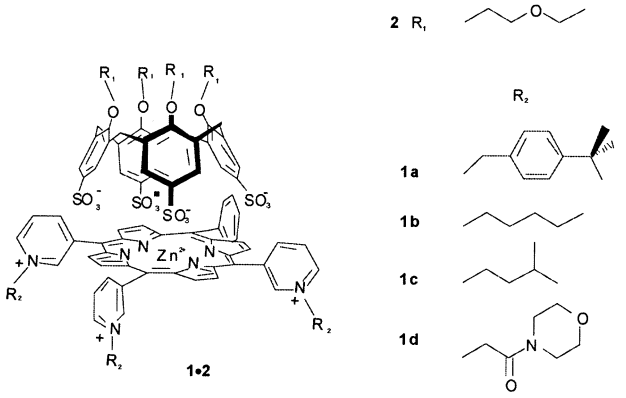

Figure 1. Molecular structures of components **1**, **2**.

Keywords: porphyrin; calix[4]arene; ionic interactions; non-covalent synthesis; molecular recognition; self-assembly.

* Corresponding authors. Tel.: +31-53-489-2980; fax: +31-53-489-4645; e-mail: p.timmerman@ct.utwente.nl

0040–4020/02/$ - see front matter
PII: S0040-4020(01)01097-3

2. Results and discussion

2.1. Synthesis

Zinc(II) *meso*-tetrakis(*N*-alkylpyridinium-3-yl) porphyrins **1a–d** were prepared by condensation of pyridine-3-carboxyaldehyde with pyrrole in a refluxing propionic acid/acetic acid (98:2) mixture followed by alkylation with excess of the appropriate alkyl bromide (chloride in case of compound **1d**) and subsequent zinc insertion ($ZnAc_2$ in MeOH, 1 h room temperature) following a known literature procedure for the preparation of compound **1b**.[19] The overall yields range from 14 to 18% thus allowing the easy preparation of the target porphyrins in gram quantities. Tetrasulfonato calix[4]arene **2** was obtained in 84% yield by sulfonation of the parent 25,26,27,28-tetrakis(2-ethoxyethoxy)calix[4]arene[20] with concentrated sulfuric acid using only half of the amount of acid reported in the reported literature procedure (for details, see Section 4).[21]

2.2. Self-assembly studies

2.2.1. UV–Vis spectroscopy. The formation of molecular assemblies **1·2** was first studied by UV–Vis spectroscopy, a suitable technique to be used in case of porphyrin-based systems. In general, titration of a solution of porphyrin **1** ($2–4\times10^{-6}$ M) with calix[4]arene **2** ($1–2\times10^{-4}$ M) in MeOH produces a bathochromic shift of the porphyrin's Soret band (3–5 nm) and a 20–25% decrease in the molar absorptivity (ϵ) at λ_{max}. A well-defined isosbestic point was clearly observed in all cases, which strongly supports the 1:1 stoichiometry of the **1·2** assemblies. Fitting of the spectral data to a 1:1 binding model afforded association constants $K_{1\cdot2}$ in the range of 10^7 M^{-1} (see Table 1). From these data it emerges that a change of the alkyl chains at the pyridyl nitrogens has almost no effect on the strength of the ion-pair complex. This result confirms our hypothesis that assembly of the 1:1 complex in MeOH is primarily driven by the cooperative formation of four salt bridges between molecular components **1** and **2**. In order to exclude that the observed spectral changes are the result of nonspecific aggregation of porphyrins **1**, the UV spectrum of porphyrin **1a** was measured at various concentrations (between 3×10^{-7} and 4×10^{-5} M in MeOH). Aggregation of the porphyrin was not observed under these conditions.

Table 1. Association constants for assemblies **1·2**

Assembly	Solvent	log $K_{1\cdot2}$	Ref.
1a·2	CH_3OH	7.11±0.04	18
1b·2	CH_3OH	7.04±0.20	18
1c·2	CH_3OH	7.15±0.09	18
1d·2	CH_3OH	6.86±0.06	This work
1d·2	H_2O/CH_3OH	5.43±0.08[a]	This work
1a·2	DMSO	6.21±0.03	18
		5.22±0.06[b]	18
		4.56±0.03[c]	18
1a·2	DMPU	6.16±0.01	18
1a·2	H_2O/DMPU	6.04±0.02	18

T=25°C, [porphyrin]=$2–3\times10^{-6}$ M (UV–Vis), 1×10^{-4} M (ITC). Given errors are standard deviations of three measurements.
[a] ITC measurement, 1×10^{-2} M Bu_4NClO_4.
[b] 1×10^{-2} M Bu_4NClO_4.
[c] 1×10^{-2} M $NaClO_4$.

Metal-free porphyrin **1a** was used to study the effect of the metal on the assembly formation. The obtained log $K_{1\cdot2}$ value for assembly formation was 8.19±0.19 M^{-1} and clearly shows that the presence of the metal ion is not a prerequisite for the observed complex formation. The even higher $K_{1\cdot2}$ value can probably be the consequence of the much higher flexibility of the metal-free porphyrin that should allow a more optimal interaction between the two moieties. This result therefore suggests that the metal center might still be available for ligand coordination and guest recognition purposes (vide infra).

2.2.2. ^{1}H NMR spectroscopy. ^{1}H NMR spectroscopy measurements in CD_3CN/D_2O mixtures were performed in order to gain structural information about complexes **1·2**. First, we studied the behavior of porphyrins **1** alone. It is well known that porphyrins like **1a** can exist in four different atropoisomeric forms (αααα, ααβ, αβαβ, and ααββ) due to the nonsymmetric substitution at the *meso* aromatic rings.[22] When the alkyl group is in the *meta* position on the *meso* pyridyl ring, atropoisomerization can occur on a time-scale comparable to the NMR chemical shift time-scale. However, the coalescence temperature can vary depending on the conditions under which the measurement is performed (presence of salts, solvent, etc.)[19] but the equilibrium remains still fast enough to prevent the physical separation of the various isomers. For porphyrin **1a** two signals were observed for the 8 β-pyrrolic protons (COSY experiments show that the two signals belong to adjacent protons) and one signal for three of the four different pyridyl protons $H_b–H_d$ (see Fig. 2) which would indicate the presence of only one isomer with fourfold symmetry. However, proton H_a exhibits a pattern more complicated than expected for just *meta* couplings with protons H_b and

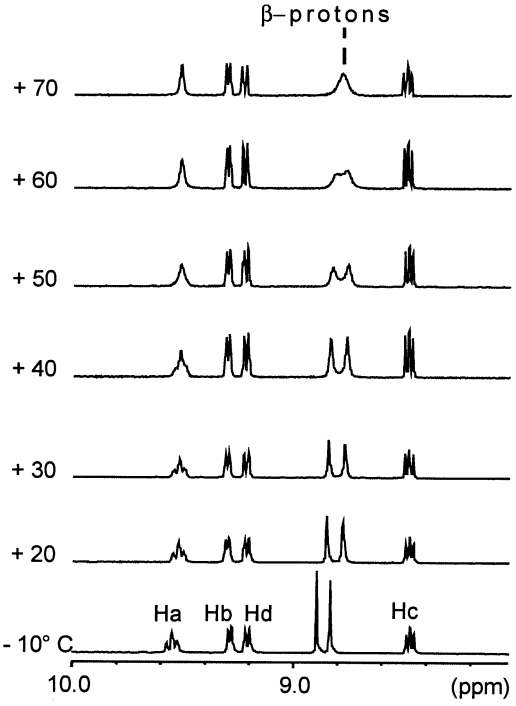

Figure 2. VT ^{1}H NMR experiments of porphyrin **1a**. Experiments were performed using 1.6 mM samples in CD_3CN/D_2O (6.5:1.5). Proton assignment as in Fig. 3.

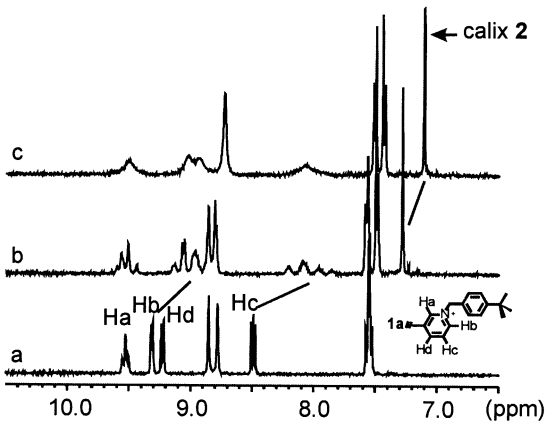

Figure 3. ^{1}H NMR of: (a) porphyrin **1a**, (b) 1:1 mixture of **1a** and **2** at 298 K, (c) at 343 K, 1.8 mm in CD_3CN/D_2O (6.5:1.5).

H_d. Moreover, VT NMR experiments showed coalescence behavior for this signal, thus ruling out the possibility of only one isomer being present. Based on this result we can conclude that porphyrin **1a** exists as a mixture of isomers presenting accidental isochronicity for most of the NMR proton signals.[22] The isomers are slowly interconverting on the NMR time scale at 25°C in CD_3CN/D_2O (6.5:1.5) and coalescence is observed around 60°C for the β-protons. Very similar ^{1}H NMR spectra were observed for porphyrins **1b**–**1d** with the β-protons also appearing as singlets or as a cluster of signals.

Subsequently, we investigated to what extent the assembly process of porphyrins **1** with calix[4]arene **2** changes their NMR spectra. For assemblies **1·2** the porphyrin proton signals always appear as a complicate set of signals at room temperature (see Fig. 3). This result agrees well with the presence of several isomers that are slowly interconverting on the NMR time scale, as observed for the free porphyrins **1**. The coalescence temperature measured for assembly **1a·2** is around 10°C higher than for **1a** alone. Ion-pair induced complexation has been observed before to affect the kinetics for atropoisomerization.[19] In this assembly the porphyrin proton signals that are most upfield shifted are relative to protons H_b, H_c, H_d, which suggests they are in closest proximity to the calix[4]arene moiety. Molecular simulation studies (CHARMm 24.0) support this interpretation. Considering for simplicity the αααα-porphyrin isomer (one of the four possible isomers present in the mixture), Fig. 4 clearly shows that the distance between the oppositely charged groups is minimal when calix[4]arene **2** approaches the porphyrin plane from the side opposite to where the alkyl groups are attached. The estimated distances $O(SO_3)$–N(alkylpyridine) are 2.74 and 3.11 Å in case the alkyl groups are pointing away or towards the calix[4]arene, respectively. In fact, porphyrin **1** is actually present as an equilibrating mixture of atropoisomers αααα, ααα**β**, αα**β**β, and α**β**α**β** in an expected statistical ratio of 1:4:2:1.[22] Nevertheless, the same considerations as mentioned for the αααα isomer would also be applicable to the ααα**β** isomer (generally the most largely present), which also has two different porphyrin faces.

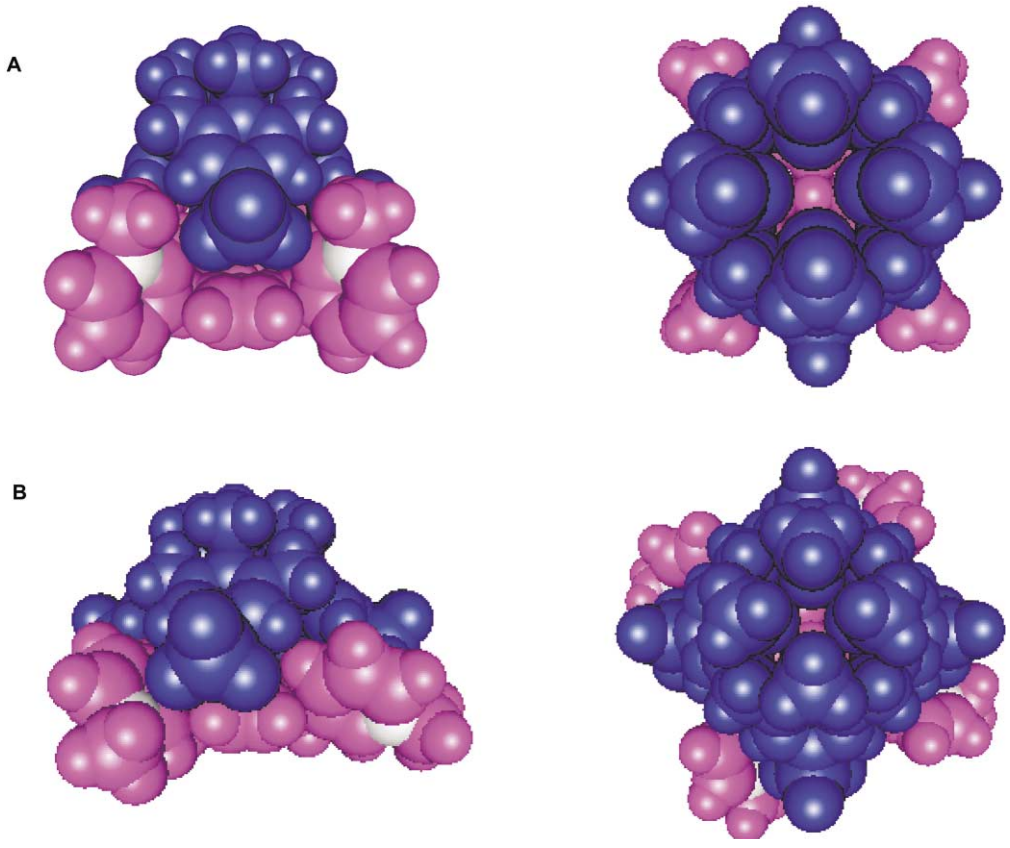

Figure 4. Molecular simulation (CHARMm 24.0) of assembly **1·2**. (**A**) *N*-alkyl groups pointing towards **2**, (**B**) *N*-alkyl groups pointing away from **2**. For simplicity, the *N*-alkyl group shown are methyls. Compound **1** is shown in gray and the pyridyl N atoms are in white; compound **2** is in blue.

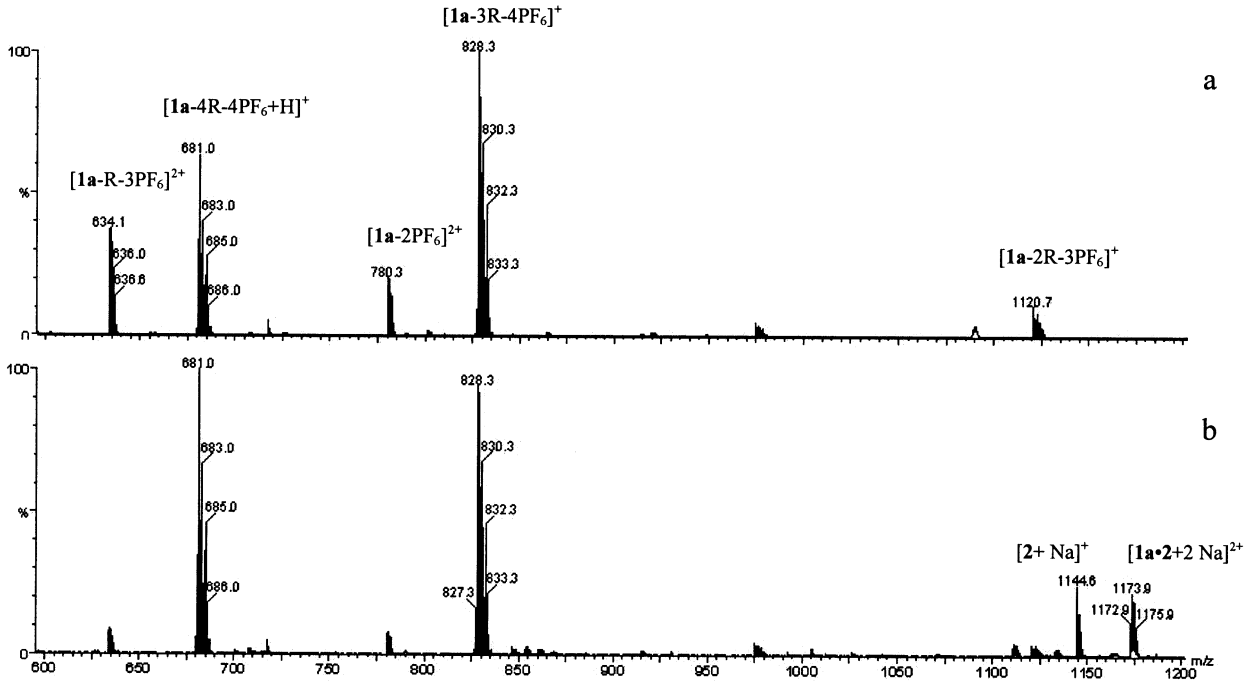

Figure 5. ESI-TOF mass spectra of (a) porphyrin **1a**, (b) assembly **1a·2**.

Small upfield shifts (0.03–0.08 ppm) were also observed for the aromatic and the methylene bridge protons of calix[4]-arene **2**, but their multiplicity was unchanged. This indicates that exchange of the components within the assembly is fast on the NMR chemical shift time scale (the lowest temperature we could access was −10°C).[†] Unfortunately, 2D ROESY experiments in CD_3CN/D_2O mixtures failed to show any crosspeak between the two building blocks. At present the reason for this is not entirely clear, but a similar observation was already reported in the case of a molecular capsule based on charged cyclodextrins in water.[23]

2.2.3. ESI-TOF mass spectrometry. Formation of assembly **1a·2** was also investigated by nano-ESI-TOF mass spectrometry.[24] Using the appropriate experimental conditions ESI-MS allows the detection of intact non-covalent complexes.[25] Analysis of an equimolar mixture of **1a** and **2** dissolved in acetonitrile and further diluted with MeOH to a 50 μM concentration showed indeed a signal at *m/z* 1173 for the doubly charged species [**1a·2**+2 Na]$^{2+}$ (Fig. 5). In addition to this, the spectrum shows two large peaks at *m/z* 681 and 828, corresponding to porphyrin **1a** that has lost four or three alkyl groups, respectively, under the mass spectrometric conditions ([**1a**-4*R*-4PF$_6$+H]$^+$ and [**1a**-3*R*-4PF$_6$]$^+$) and a third peak at *m/z* 1144 corresponding to free calix[4]arene [**2**+Na]$^+$. Other small peaks are also present at *m/z* 634 and 780 for the monodealkylated species [**1a**-*R*-3PF$_6$]$^{2+}$ and for the intact porphyrin [**1a**-2PF$_6$]$^{2+}$. ESI-TOF-MS analysis of a sample of porphyrin **1a** alone showed also the same dealkylation pattern. Attempts to study the ion-pair complex formation by MALDI-TOF MS were not successful and we could only detect the two peaks corresponding to completely or largely dealkylated porphyrin: [**1a**-4*R*-4PF$_6$+H]$^+$ and [**1a**-3*R*-4PF$_6$]$^+$.

2.2.4. Enthalpic and entropic contribution to the binding process. In order to get a better understanding of the assembly process, we have determined the thermodynamic parameters associated with the complex formation, either using variable temperature UV–Vis titration experiments or isothermal titration microcalorimetry (ITC) measurements (Table 2). In pure MeOH, the formation of assembly **1a·2** did not show any appreciable heat effect in an attempted ITC measurement, thus preventing the use of this powerful technique in this specific case. The thermodynamic parameters were thus indirectly determined by van't Hoff analysis of VT UV-studies. The low enthalpy measured (especially if the error of the determination is considered) is in reasonable agreement with the ITC observation. The process is therefore almost entirely entropy driven. However, in MeOH/H_2O mixture (x_w=45%) with Bu_4NClO_4 (1×10^{-2} M) as support electrolyte, the system produces an appreciable heat effect. As a result of the more polar nature of porphyrin **1d**, the formation of assembly **1d·2** could be conveniently studied in this medium via ITC measurements (see Fig. 6). The assembly formation is still strongly entropically driven (148±3 J K^{-1} mol^{-1}).

Table 2. Thermodynamic parameters for the formation of **1·2**

Assembly	Solvent	ΔH (kJ mol^{-1})	ΔS (J mol^{-1} K^{-1})
1a·2	MeOH	−8.0±6.7[a]	+129±24[a]
1d·2	MeOH/H_2O (x_w=0.45)	+13.2±0.4[b]	+148±3[b]

[Porphyrin]=2–3×10^{-6} M (UV–Vis), 1×10^{-4} M (ITC).
[a] VT UV, $K_{1\cdot2}$ measured at 7 different temperatures. Errors are standard deviations obtained from the linear regression.
[b] ITC, 25°C, 1×10^{-2} M Bu_4NClO_4. Errors are standard deviations of three measurements.

[†] Below −10°C the D_2O/CD_3CN solvent mixture separates into two different phases.

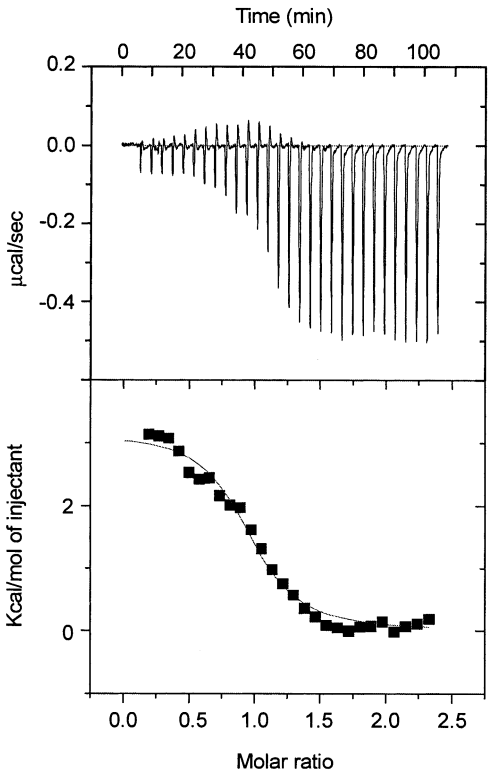

Figure 6. ITC titration showing the heat evolved per injection of titrant as a function of assembly building blocks ratio ([**1d**]/[**2**]).

aprotic solvents, like DMSO and DMPU (1,3-dimethyl-3,4,5,6-tetrahydropyrimidin-2(1*H*)-one), the association constant $K_{\mathbf{1}\cdot\mathbf{2}}$ is around 10 times smaller than in MeOH. A similar value was also obtained when water was added to DMPU (x_w=0.26). These results indicate that MeOH is the superior solvent for assembly formation and suggest a stabilizing effect due to the use of MeOH, possibly related to the inclusion of one (or two hydrogen-bonded[26]) solvent molecules within the assembly cavity. This conclusion is also supported by molecular simulation studies that confirm that one MeOH molecule can be accommodated without any distortion of the cavity (see Fig. 7).‡

When stability measurements were performed in DMSO in the presence of 10^{-2} M Bu_4NClO_4 (4500 times the concentration of the building blocks), $K_{\mathbf{1}\cdot\mathbf{2}}$ was observed to decrease only 10 times in comparison to the pure solvent. However, in the presence of 10^{-2} M $NaClO_4$ a 45-time decrease in association constant was obtained. A more detailed study of $K_{\mathbf{1}\cdot\mathbf{2}}$ as a function of the $NaClO_4$ concentration showed that the effect is probably due to a specific interaction of the Na^+ cation with calix[4]arene **2**. A logarithmic plot of $K_{\mathbf{1}\cdot\mathbf{2}}$ vs [$NaClO_4$] shows a bimodal linear dependence of $K_{\mathbf{1}\cdot\mathbf{2}}$ with a slope of 1.91±0.11 for [$NaClO_4$]>2×10^{-3} M (Fig. 8), suggesting weak binding of two Na^+ ions (β=2.2×10^5 M^{-2}) most likely to the lower rim of the calix[4]-arene unit. The complexation appears to be cooperative as indicated by the sharp curvature at the breaking point. In terms of molecular structure, the observed cooperativity is

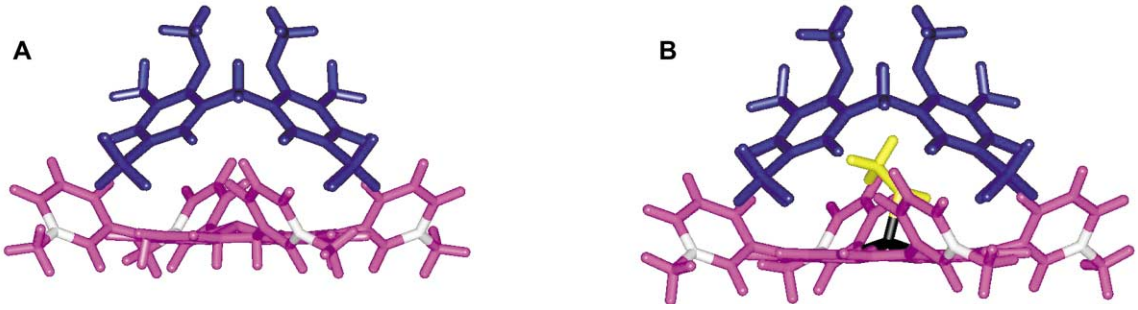

Figure 7. Molecular simulation (CHARMm 24.0) of assembly **1·2**: (A) empty cavity, (B) cavity filled with MeOH. For simplicity, the *N*-alkyl group shown are methyls.

The positive enthalpy change observed in this case (13.2±0.4 kJ mol^{-1}) must arise from a positive enthalpy of desolvation, which overrides the expected negative enthalpy for complex formation. The observed $K_{\mathbf{1}\cdot\mathbf{2}}$ in this solvent mixture is 27 times smaller than that in pure MeOH, reflecting the weakening of electrostatic interactions in a solvent mixture with higher dielectric constant containing 100 equiv. of Bu_4NClO_4.

2.2.5. Solvent and salt effects. The stability of complexes **1·2** was then investigated in different polar solvents and in the presence of added salts. The complexes remain stable in a range of polar solvents with a degree of complexation ≥95% at millimolar concentration (Table 1). In all cases UV–Vis titration experiments with **1a** and **2** gave well-defined isosbestic spectral changes, confirming clearly the 1:1 stoichiometry of the complexes in all solvents. In polar most probably attributable to the preorganization of the ethoxy–ethoxy chains after the first Na^+ ion has been complexed to the lower rim oxygens.

2.3. Ligand binding studies

We have also studied the coordination of axial ligands **L** to the zinc center of assembly **1a·2** to give ternary complexes **1a·2·L**. Zinc porphyrins are known to bind only one axial ligand molecule and therefore represent the simplest model system to study axial coordination to metallo porphyrins.

‡ Also for these molecular simulation studies only the αααα isomer has been considered. Under this assumption, we have obtained that bulkier solvents like DMSO and DMPU might be less efficient in filling the cavity because they cause a distortion of the **1·2** complex.

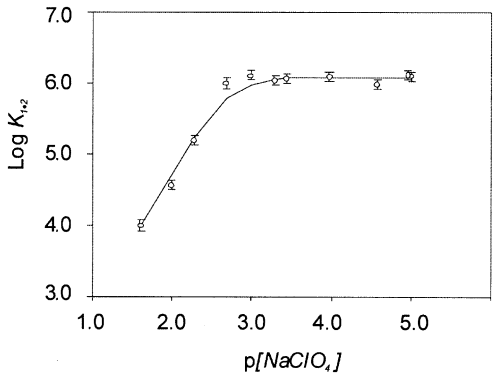

Figure 8. Effect of the presence of $NaClO_4$ on the strength of formation of assembly **1a·2**.

UV–Vis titration experiments using 1-methylimidazole or pyridine as axial ligands (**L**), clearly showed the formation of the expected ternary complexes **1a·2·L**. The observed spectral changes in the Q bands region (see Fig. 9) were fitted to a 1:1:1 equilibrium model in order to obtain values for the equilibrium constant $K_{1\cdot2\cdot L}$ (see Eqs. (1)–(3))

$$\mathbf{1} + \mathbf{2} \leftrightharpoons \mathbf{1{\cdot}2} \qquad K_{1\cdot2} \tag{1}$$

$$\mathbf{1} + \mathbf{L} \leftrightharpoons \mathbf{1{\cdot}L} \qquad K_{1\cdot L} \tag{2}$$

$$\mathbf{1} + \mathbf{2} + \mathbf{L} \leftrightharpoons \mathbf{1{\cdot}2{\cdot}L} \qquad K_{1\cdot2\cdot L} \tag{3}$$

The strength of coordination of the axial ligand **L** to porphyrin **1** ($K_{1\cdot L}$ in Eq. (2)) was determined in a separate

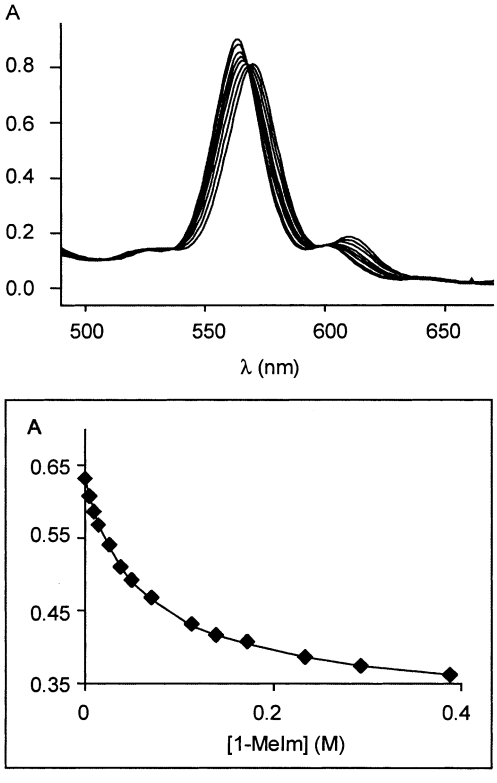

Figure 9. Spectral evolution of a 1:1 mixture of porphyrin **1a** and calix **2** in MeOH (4×10^{-5} M, assembly **1a·2** present >95%) titrated with 1-methylimidazole (1-MeIm). The lower part shows the fitting of the titration curve at 555 nm.

Table 3. Complexation of ligands by porphyrin **1a** and assembly **1a·2**

	1-MeIm		Pyridine	
	$K_{1\cdot2\cdot L}/K_{1\cdot2}$ (M^{-1})	$K_{1\cdot L}$ (M^{-1})	$K_{1\cdot2\cdot L}/K_{1\cdot2}$ (M^{-1})	$K_{1\cdot L}$ (M^{-1})
DMSO	53±1	53±1	n.d.	n.d.
MeOH	17.0±0.5	62±1	2.0±0.2	5.9±0.1

T=25°C, [porphyrin]=[calix]=3–4×10^{-5} M (UV–Vis). Given errors are standard deviations of three measurements.

experiment. The ratio $K_{1\cdot2\cdot L}/K_{1\cdot2}$ represents the ligand affinity displayed by assembly **1·2**. The results reported in Table 3 clearly show that $K_{1\cdot2\cdot L}/K_{1\cdot2} \leq K_{1\cdot L}$, which indicates that no cavity effect is observed. Two main reasons should be considered to interpret this observation: (i) the cavity is too small to accommodate the ligand, (ii) or the cavity is occupied by solvent molecules and there is not a very strong enthalpic effect for the ligand to drive the encapsulation process. The first option seems improbable if it is considered that the absence of directionality in ion-pair interactions and their weak dependence on distance (proportional to r^1),[27] should result in assemblies that present a poorly defined cavity able to encapsulate either solvent molecules or the desired guest. The second option is therefore the most likely explanation: MeOH is in fact the solvent in which the largest drop in binding strength for a given ligand **L** is observed ($K_{1\cdot2\cdot L}/K_{1\cdot2} \leq 1/3\ K_{1\cdot L}$,). This result is in agreement with the fact that it was found to be the best solvent for the assembly formation, possibly due to a reasonably strong template effect. The systems **1·2** thus behave very differently from related covalently linked calix[4]arene capped porphyrins[28] that show increased binding affinities in comparison to the non-capped model porphyrins. This is probably a consequence of the very different rigidity and shape-selectivity between the two systems.

We are now exploring the possibility of using the highly dynamic nature of this assembly together with their peculiar ligand recognition properties for catalytic application. We are also starting the investigation of related systems in pure water. The recognition properties of the assembly are then expected to change according to the importance of hydrophobic interactions in aqueous media.

3. Conclusions and outlook

We have reported the high thermodynamic stability of non-covalent calix[4]arene-capped porphyrins in polar solvents and in organic solvent/water mixtures with as much as 45% molar fraction of water. The systems remain remarkably stable even upon addition of an excess of electrolyte.

We think that these results can be easily extended to other and even more complicate systems. The application of ionic interactions for the self-assembly of supramolecular structures is a very interesting approach mainly for two reasons: is low synthetic demanding and it is possible to work in solvents that are usually not accessible for structures obtained by hydrogen bonding. It seems likely that the same approach can be extended to systems in pure water

thus allowing the study of models for biologically occurring porphyrins under physiological conditions.

4. Experimental

4.1. General information and instrumentation

All reagent used were purchased from Aldrich or Acros Organics and used without further purification. All the reactions were performed under nitrogen atmosphere. Infrared spectra were recorded on a FT-IR Perkin Elmer Spectrum BX spectrometer and only characteristic absorptions are reported. ^{1}H and ^{13}C NMR spectra were performed on a Varian Unity INOVA (300 MHz) or a Varian Unity 400 WB NMR spectrometer. ^{1}H NMR chemical shift values (300 MHz) are expressed in ppm (δ) relative to residual CHD_2OD (δ 3.30), CHD_2CN (δ 1.93), or $CHCl_3$ (δ 7.26). ^{13}C NMR chemical shift values (100 MHz) are expressed in ppm (δ) relative to residual CD_3OD (δ 49.0) or CD_3CN (δ 1.3). UV–Vis measurements were performed on a Varian Cary 3E UV–Vis spectrophotometer equipped with a Helma QX optical fiber probe (path length=1.000 cm), using solvents of spectroscopic grade. Calorimetric measurements were carried out using a Microcal VP-ITC microcalorimeter with a cell volume of 1.4115 mL. Elemental analyses were carried out using a 1106 Carlo–Erba Strumentazione element analyzer. Compound **1b** was prepared according to literature.[19]

4.2. Binding studies

UV–Vis: Association constants for assemblies **1**·**2** were evaluated by measuring the absorbances changes upon addition of increasing amount of a calix[4]arene **2** solution to a porphyrin **1** solution ($2–3\times10^{-6}$ M). Each titration consisted of 15–20 additions. The calix[4]arene solution was at a concentration high enough so that the degree of complexation during the titration was between about 20 and 80%, and the overall dilution was less than 3%. The experimental spectral changes were fitted to a 1:1 binding model using a non-linear least squares fitting procedure[29] that considered the information coming from 6 different wavelengths (model written with program Scientist®, MicroMath®). In a similar way were determined the binding constants for axial ligands.

4.3. ESI-TOF mass spectrometry

Electrospray ionization mass spectra were recorded on a Micromass LCT time-of-flight mass spectrometer. Samples were introduced using a nanospray source.

4.4. Molecular modeling calculations

Molecular simulation studies were carried out as described elsewhere.[30]

4.5. General procedure for the preparation of [5,10,15,20-tetrakis(*N*-alkylpyridinium-3-yl)porphyrinato]-zinc(II) (1)

A solution of 5,10,15,20-tetra(3-pyridyl)porphyrin (100 mg, 0.161 mmol) and the suitable alkylbromide (100–200 equiv.) in DMF (30–50 mL) was stirred for 8–17 h at 80°C, analogous to a literature procedure.[19] The reaction was monitored by TLC (silica gel $60F_{254}$, CH_3CN/(3 mg/mL of NH_4PF_6 in H_2O) 7:3). After removal of the DMF, the residue was triturated with diethyl ether and subsequently dried under vacuum. The crude product is sufficiently clean (based on ^{1}H NMR) to be used in subsequent reactions. Purification of an analytical sample was performed by dissolving the material in MeOH and precipitating **1** by addition of a solution of NH_4PF_6 in water. The precipitate was filtered off and washed extensively with water and ether. The corresponding chloride salt of **1a** was obtained by passing the PF_6 salt through an ion-exchange column (DOWEX 1-X8, 50–100 mesh, Cl-form) using CH_3CN/H_2O 1:1 v/v as the eluent.

Insertion of the Zn was carried out by stirring the alkylated porphyrin in MeOH saturated with $ZnAc_2$ at room temperature for 1 h, after which a solution of NH_4PF_6 in water was added to precipitate the metallated porphyrin **1**. The solid was filtered off and washed extensively with water and ether.

4.5.1. 5,10,15,20-Tetrakis(*N*-*p*-*t*-butylbenzylpyridinium-3-yl)porphyrin (1a-free base). Yield: 85%. The compound was fully characterized as the chloride salt. ^{1}H NMR (CD_3OD) δ 10.10 (m, 4H), 9.58 (d, J=6.0 Hz, 4H), 9.44 (d, J=7.9 Hz, 4H), 9.07 (br s, 8H), 8.61 (m, 4H), 7.65 (m, 16H), 6.18 (s, 8H), 1.34 (s, 36H); ^{13}C NMR δ 154.86, 150.40, 148.32, 145.79, 143.24, 131.71, 130.32, 128.47, 127.88, 114.41, 66.19, 35.73, 31.64; IR (KBr) 3414, 3068, 2962, 2868, 1628, 1499, 1465, 1196, 979, 794; UV–Vis (MeOH) 422, 512, 544, 586, 643; Anal. Calcd for $C_{84}H_{86}N_8Cl_4\cdot9H_2O$: C, 66.75; H, 6.93; N, 7.41; Found: C, 66.85; H, 6.57; N, 7.30.

Hexafluorophosphate salt: ^{1}H NMR (CD_3CN) δ 9.56 (m, 4H), 9.26 (m, 8H), 9.00 (s, 4H), 8.94 (s, 4H), 8.52 (t, J=7.0 Hz, 4H), 7.58 (m, 16H), 6.02 (s, 8H), 1.30 (s, 36H), −3.15 (s, 2H).

4.5.2. [5,10,15,20-Tetrakis(*N*-*p*-*t*-butylbenzylpyridinium-3-yl)porphyrinato]zinc(II) (1a). Yield: 80% (alkylation+metallation). ^{1}H NMR (CD_3OD) δ 9.93 (m, 4H), 9.48 (m, 4H), 9.35 (d, J=7.7 Hz, 4H), 8.99 (s, 4H), 8.93 (s, 4H), 8.54 (t, J=7.0 Hz, 4H), 7.64 (m, 16H), 6.13 (s, 8H), 1.33 (s, 36H); UV–Vis (MeOH) 433, 521, 560, 596; Anal. Calcd for $C_{84}H_{84}N_8P_4F_{24}Zn$: C, 54.51; H, 4.57; N, 6.05, Found: C, 54.15; H, 4.49; N, 5.91.

4.5.3. [5,10,15,20-Tetrakis(*N*-(3-methylbutyl)pyridinium-3-yl)porphyrinato]zinc(II) (1c). Yield: 91% (alkylation+metallation). ^{1}H NMR (CD_3CN) δ 9.53 (m, 4H), 9.20 (m, 8H), 9.00 (m, 8H), 8.47 (t, J=7.0 Hz, 4H), 4.85 (t, J=7.8 Hz, 8H), 2.15 (m, 8H), 1.87 (sept, J=6.5 Hz, 4H), 1.05 (d, J=6.5 Hz, 24H); ^{13}C NMR δ 151.36, 149.52, 147.09, 145.11, 143.96, 133.99, 128.02, 114.26, 62.02,

40.96, 26.80, 22.58; IR (KBr) 3107, 2960, 2875, 1629, 1498, 1200, 1159, 843, 558; UV–Vis (MeOH) 431, 520, 559, 597, 633; Anal. Calcd for $C_{60}H_{68}N_8F_{24}P_4Zn$: C, 46.60; H, 4.43; N, 7.25; Found: C, 46.41; H, 4.29; N 7.33.

4.5.4. [5,10,15,20-Tetrakis(*N*-(4-glycylmorpholyl)pyridinium-3-yl) porphyrin (1d). 5,10,15,20-tetra(3-pyridyl)-porphyrin (200 mg, 0.323 mmol) and chloroacetylmorpholine (240 mg, 1.45 mmol) were dissolved in acetonitrile (30 mL). NaI (218 mg, 1.45 mmol) was added and the mixture was refluxed for 21 h. The solvent was then removed under vacuum and the residue triturated with ether and redissolved in MeOH. The product was precipitated by addition of NH_4PF_6 in water, filtered off and washed with water and ether to afford crude alkylated porphyrin in 91% yield (0.28 mmol, 502 mg). Metallation with $ZnAc_2$ as previously described, afforded **1d** as a purple solid in 85% yield (0.27 mmol, 485 mg).

^{1}H NMR (CD_3CN) δ 9.26 (m, 4H), 9.17 (d, J=8.0 Hz, 4H), 8.91 (s, 12H), 8.36 (t, J=7.0 Hz, 4H), 5.63 (s, 8H), 3.63–3.36 (m, 32H); ^{13}C NMR δ 164.02, 151.33, 150.43, 149.24, 146.21, 143.00, 133.97, 127.47, 114.17, 67.201, 66.96, 62.96, 46.17, 43.87; IR (KBr) 3101, 2932, 2866, 1661, 1450, 1246, 1112, 842, 558; UV–Vis (MeOH) 432, 520, 559, 596, 636; Anal. Calcd for $C_{64}H_{64}N_{12}O_8F_{24}P_4Zn$: C, 43.32; H, 3.64; N, 9.47; Found: C, 43.31; H, 3.42; N 9.42.

4.5.5. 5,11,17,23-Tetrasulfonato-25,26,27,28-tetrakis(2-ethoxyethoxy)calix[4]arene, tetrasodiumsalt (2).[21] 25,26,27,28-Tetrakis(2-ethoxyethoxy)calix[4]arene[20] (2.00 g, 2.80 mmol) was dissolved in concentrated H_2SO_4 (96%, 5 mL) and stirred at room temperature for 2 h. The reaction mixture was then quenched by pouring it carefully into water and neutralized by addition of a concentrated solution of NaOH (~5 M). The water was then removed under reduced pressure and the solid residue was extracted overnight using a Soxhlet extractor with MeOH. The crude product was then purified by reversed phase chromatography (Merck Lobar column, LiChroprep RP8, 40–63 μm) eluting initially with pure water until no more inorganic sulfates were detected (no precipitation observed upon addition of $BaCl_2$ to the eluate). Pure **2** was then obtained by elution in a step-gradient to 70% EtOH/H_2O (v/v). After concentration under vacuum to remove most of the ethanol, the remaining water was removed by freeze-drying to afford **2** as a white solid in 84% yield (2.36 mmol, 2.65 g).

Acknowledgements

We thank Professor Feike de Jong for helpful discussion. These investigations are supported by the Netherlands Research Council for Chemical Sciences (CW) with financial aid from the Technology Foundation STW.

References

1. *Biochemistry*, Stryer, H., Ed.; 4th ed, Freeman: New York, 1995; p. 23.
2. Ortiz de Montellano, P. R. *Cytochrome P-450: Structure, Mechanism and Biochemistry*; 2nd ed; Plenum: New York, 1995.
3. Everse, J., Everse, K. E., Grisham, M. P., Eds.; *Peroxidases in Chemistry and Biology*, CRC: Boca Raton, FL, 1991; Vols. I and II.
4. Feiters, M. C. *Comprehensive Supramolecular Chemistry*; Atwood, J. L., Davies, J. E. D., MacNicol, D. D., Vögtle, F., Reinhoudt, D. N., Lehn, J.-M., Eds.; Elsevier: Elmsford, 1996; Vol. 10, pp. 267–360.
5. Momenteau, M.; Reed, C. A. *Chem. Rev.* **1994**, *94*, 659–698.
6. Jones, R. D.; Summerville, D. A.; Basolo, F. *Chem. Rev.* **1979**, *79*, 139–179.
7. Wojaczynski, J.; Latos-Grazynski, L. *Coord. Chem. Rev.* **2000**, *204*, 113–171.
8. Drain, C. M.; Russel, K. C.; Lehn, J.-M. *Chem. Commun.* **1996**, 337–338.
9. Ruhlmann, L.; Nakamura, A.; Vos, J. G.; Fuhrhop, J.-H. *Inorg. Chem.* **1998**, *37*, 6052.
10. Yamamoto, K.; Nakazawa, S.; Matsufuji, A.; Taguchi, T. *J. Chem. Soc., Dalton Trans.* **2001**, 251–258.
11. Sirish, M.; Schneider, H.-J. *Chem. Commun.* **2000**, 23–24.
12. Zhao, S.; Luong, J. H. T. *J. Chem. Soc., Chem. Commun.* **1995**, 663–664.
13. Ribò, J. M.; Farrera, J.-A.; Valero, M. L.; Virgili, A. *Tetrahedron* **1995**, *51*, 3705–3712.
14. Manka, J. S.; Lawrence, D. S. *J. Am. Chem. Soc.* **1990**, *112*, 2440–2442.
15. Lahiri, J.; Fate, G. D.; Ungashe, S. B.; Groves, J. T. *J. Am. Chem. Soc.* **1996**, *118*, 2347–2358.
16. Tecilla, P.; Dixon, R. P.; Slobodkin, G.; Alavi, D. S.; Waldeck, D. H.; Hamilton, A. D. *J. Am. Chem. Soc.* **1990**, *112*, 9408–9410.
17. Takeuchi, M.; Kijima, H.; Hamachi, I.; Shinkai, S. *Bull. Chem. Soc. Jpn* **1997**, *70*, 699–705.
18. Fiammengo, R.; Timmerman, P.; de Jong, F.; Reinhoudt, D. N. *Chem. Commun.* **2000**, 2313–2314.
19. Mizutani, T.; Horiguchi, T.; Koyama, H.; Uratani, I.; Ogoshi, H. *Bull. Chem. Soc. Jpn* **1998**, *71*, 413–418.
20. Arduini, A.; Casnati, A.; Fabbi, M.; Minari, P.; Pochini, A.; Sicuri, A. R.; Ungaro, R. *Supramol. Chem.* **1993**, *1*, 235–246.
21. Casnati, A.; Ting, Y.; Berti, D.; Fabbi, M.; Pochini, A.; Ungaro, R.; Sciotto, D.; Lombardo, G. G. *Tetrahedron* **1993**, *49*, 9815–9822.
22. Crossley, M. J.; Field, L. D.; Forster, A. J.; Harding, M. M.; Sternhell, S. *J. Am. Chem. Soc.* **1987**, *109*, 341–348.
23. Hamelin, B.; Jullien, L.; Derouet, C.; Hervé du Penhoat, C.; Berthault, P. *J. Am. Chem. Soc.* **1998**, *120*, 8438–8447.
24. Brody, M. S.; Schalley, C. A.; Rudkevich, D. M.; Rebek, Jr., J. *Angew. Chem., Int. Ed. Engl.* **1999**, *38*, 1640–1644.
25. Staroske, T.; O'Brien, D. P.; Jørgensen, T. J. D.; Roepstorff, P.; William, D. H.; Heck, A. J. R. *Chem. Eur. J.* **2000**, *6*, 504–509.
26. Bonar-Law, R. P.; Sanders, J. K. M. *J. Am. Chem. Soc.* **1995**, *117*, 259–271.
27. Hossain, M. A.; Schneider, H.-J. *Chem. Eur. J.* **1999**, *5*, 1284–1290.
28. Rudkevich, D. M.; Verboom, W.; Reinhoudt, D. N. *J. Org. Chem.* **1995**, *60*, 6585–6587.
29. Leggett, D. J.; Kelly, S. L.; Shiue, L. R.; Wu, Y. T.; Chang, D.; Kadish, K. M. *Talanta* **1983**, *30*, 579–586.
30. Timmerman, P.; Weidmann, J.-L.; Jolliffe, K. A.; Prins, L. J.; Reinhoudt, D. N.; Shinkai, S.; Frish, L.; Cohen, Y. *J. Chem. Soc., Perkin Trans. 2* **2000**, 2077–2089.